Measurements and modeling of photolysis rates during the Photochemical Activity and Ultraviolet Radiation (PAUR) II campaign

D. S. Balis,[1] C. S. Zerefos,[1] K. Kourtidis,[1] A. F. Bais,[1] A. Hofzumahaus,[2] A. Kraus,[2,3] R. Schmitt,[4] M. Blumthaler,[5] and G. P. Gobbi[6]

Received 6 November 2000; revised 15 June 2001; accepted 18 June 2001; published 11 September 2002.

[1] In this paper we compare radiative transfer model calculations of the actinic flux in the UV spectral region with airborne measurements of the actinic flux, obtained during the Photochemical Activity and Ultraviolet Radiation (PAUR) campaign, which took place in the Aegean Sea, Greece, in June 1996, in order to assess the accuracy of the model in calculating photolysis rates, when the model input parameters are well defined from measurements. The model can simulate the total actinic flux (4π sr) in the UV-A region with an accuracy of 5% for all altitudes (0.1–12 km) in the cloud free troposphere, while in the UV-B the impact of the vertical distribution of ozone and aerosol can lead to differences, of about 5–10% at low altitudes up to 20% at higher altitudes. Next, the photolysis rates of $J(O^1D)$ and $J(NO_2)$ measured during the PAUR 2, in Crete, Greece (35.5°N, 23.8°E), in May 1999, at two altitudes (Gerani 30 m and Prases 1000 m), are compared with the respective model calculations in order to examine the effect of the alternating Sahara dust/maritime aerosol environments imposed to these photolysis rates, as well as to examine their differences due to the altitude difference. It is shown that high levels of tropospheric ozone and absorbing aerosols can cause a decrease in the photolysis rates of ozone near the surface, even under conditions of reduced total ozone content. This fact indicates that tropospheric ozone can be disproportionately important as a filter against UV-B radiation when most scattering of the radiation by air molecules and dust occurs in the troposphere. This behavior is not simulated accurately using a radiative transfer model constrained by observations of ozone and aerosol optical depths. The differences of the of the photolysis rates between the two altitudes as determined by the model and by the measurements, differ significantly for the Sahara dust event, indicating that during this event in the boundary layer, there is a mixture of desert and nonabsorbing aerosols. *INDEX TERMS:* 0365 Atmospheric Composition and Structure: Troposphere—composition and chemistry; 0368 Atmospheric Composition and Structure: Troposphere—constituent transport and chemistry; 0317 Atmospheric Composition and Structure: Chemical kinetic and photochemical properties; *KEYWORDS:* Total ozone, photochemistry, UVB radiation

Citation: Balis, D. S., C. S. Zerefos, K. Kourtidis, A. F. Bais, A. Hofzumahaus, A. Kraus, R. Schmitt, M. Blumthaler, and G. P. Gobbi, Measurements and modeling of photolysis rates during the Photochemical Activity and Ultraviolet Radiation (PAUR) II campaign, *J. Geophys. Res.*, *107*(D18), 8138, doi:10.1029/2000JD000136, 2002.

1. Introduction

[2] The knowledge of the photolysis rates of key atmospheric compounds is of considerable importance for the atmospheric chemistry. The photolysis of ozone (O_3) into O^1D in the presence of water vapor is the main source of hydroxyl radicals (OH), which determine the oxidizing capacity of the atmosphere and thus the lifetime of many tropospheric gases. The photolysis of nitrogen dioxide (NO_2) controls the photochemical production of ozone and the concentrations of the total peroxy radicals. The photolysis rate coefficients are an essential input to photochemical models of the atmosphere. The photolysis rate of a given molecule can be calculated from

$$J = \int \sigma(\lambda, T)\phi(\lambda, T)F(\lambda)d\lambda, \quad (1)$$

where $\sigma(\lambda, T)$ is the wavelength- and temperature-dependent absorption cross section of the molecule, $\Phi(\lambda, T)$ is the

[1]Laboratory of Atmospheric Physics, Aristotle University of Thessaloniki, Greece.
[2]Institute for Atmospheric Chemistry, Forschungzentrum Jülich, Germany.
[3]Now at Gruenenthal GmbH, Aachen, Germany.
[4]Meteorologie Consult GmbH, Hessen, Germany.
[5]Institute of Medical Physics, University of Innsbruck, Innsbruck, Austria.
[6]Instituto di Fisica Dell' Atmosfera, Consiglio Nazionale delle Ricerche, Rome, Italy.

0148-0227/02/2000JD000136

quantum yield of the molecule and $F(\lambda)$ is the solar actinic flux for a certain zenith angle and altitude, determined as [e.g., *Madronich*, 1993]

$$F = F_{dir}/\mu_0 + \int_0^{2\pi}\int_{-1}^{+1} I(\vartheta,\varphi)d(\cos\vartheta)d\varphi, \qquad (2)$$

where F_{dir} is the direct component of the actinic flux, μ_0 is the cosine of the solar zenith angle, I is the spectral radiance (or intensity), and θ and φ are the polar and azimuthal angles of the diffuse radiance.

[3] The absorption cross section and the quantum yield are measured experimentally in the laboratory, while the actinic flux over the spectral region of interest can be either measured in the field or calculated theoretically, using a radiative transfer model. The photolysis of NO_2 occurs for $\lambda < 420$ nm, while the photolysis of O_3 occurs for $\lambda < 330$ nm. The well-established negative stratospheric ozone trends [e.g., *World Meteorological Organization*, 1999] and the strong indications for increases of the solar UV irradiance, reaching the Earth's surface [e.g., *Zerefos et al.*, 1997, 1998a; *Seckmeyer et al.*, 1997; *Kerr and McElroy*, 1993], suggest that the accurate knowledge of these photolysis rates will be essential for modeling and predicting the impact of the above mentioned changes to the tropospheric chemistry.

[4] There have been various studies, either experimental or theoretical, which cover different aspects of the accurate determination of photolysis rates. Most of these studies refer to measurement campaigns, laboratory studies, and radiative transfer modeling. For a long time, measurements of photolysis frequencies were performed using chemical actinometry [e.g., *Lantz et al.*, 1996; *Shetter et al.*, 1996, and references therein]. *Müller et al.* [1995] presented a new experimental approach for the determination of the photolysis rate of ozone from spectroradiometric measurements and compared them with chemical actinometer measurements. They performed their measurements at ground in Jülich, Germany, in the fall of 1993. The field comparison indicated the importance of accurate measurements of the O^1D quantum yield and supported laboratory studies where they measured O^1D quantum yields of 0.2 to 0.3 between 315 and 320 nm. *McElroy et al.* [1995] determined photolysis frequencies from airborne measurements of direct and scattered solar irradiance. They compared the J values with model calculations, using the same absorption cross sections and quantum yields for measurement and found agreement within 20% for $J(NO_2)$ and $J(O^1D)$. An accuracy of 10% was also found by *Kraus et al.* [2000] for the spectroradiometric determination of $J(NO_2)$ during the JCOM97 experiment. Within the experimental uncertainties, *Kraus and Hofzumahaus* [1998] found good agreement between photolysis rates determined by spectroradiometry and those determined by filter radiometers, absolutely calibrated against chemical actinometers. *Lantz et al.* [1996] determined theoretically, as well as with radiometric and actinometric means, the photolysis rate coefficient of NO_2 during the Mauna Loa Observatory Photochemistry Experiment 2 (MLOPEX 2) and found a discrepancy between theoretical and measured values of the order of 40%, which could not be attributed to any changes of an aerosol indicator. *Shetter et al.* [1996], also during MLOPEX 2, performed radiometric and actinometric measurements of the $J(O^1D)$, along with modeling calculations. They confirmed the importance of the accurate experimental determination of the quantum yield, which affects the comparison between theoretical and measured values. A number of groups [*Michelsen et al.*, 1994; *Takahashi et al.*, 1996; *Ball et al.*, 1997; *Silvente et al.*, 1997; *Talukdar et al.*, 1998] remeasured the O^1D quantum yield in the laboratory. *Talukdar et al.* [1998] presented measurements of the O^1D quantum yields between 203 K and 320 K and 289 to 329 nm and calculated larger photolysis rates than those obtained from previous recommendations [*Atkinson et al.*, 1992; *DeMore et al.*, 1994] also depending on the solar zenith angle and ozone column abundance.

[5] The need for accurate photolysis rates in photochemical modeling resulted in the development of various radiative transfer models, which calculate these rates. There are recently many sensitivity studies, which use these models to examine the influence of various input parameters in the calculated photolysis rates and in photochemical activity. *Madronich and Granier* [1994] note that increases in tropospheric UV, resulting from stratospheric ozone depletion will increase the reactivity of the troposphere. *Krol and van Weele* [1997] studied the effect of ozone depletion, clouds, and surface reflection on photolysis rates and their implications for global atmospheric chemistry, indicating that stratospheric ozone affects predominately the photolysis rate of ozone, while clouds and surface reflectivity affect all photolysis rates. *Castro et al.* [1997] provided a sensitivity analysis of photolysis rates of NO_2 in the atmosphere of Mexico City and highlighted the importance for providing local resolution for photolysis rates by considering different local conditions within the modeling domain of air quality models. *Ruggaber et al.* [1997] used their radiative transfer model to calculate photolysis rates in the aqueous phase, which play an important role in atmospheric chemistry. *Jacobson* [1998] studied the effects of aerosols on vertical photolysis rate coefficients over an urban air shed, indicating that photolysis rate changes due to aerosols decreased near-surface ozone mixing ratios in Los Angeles by 5–8%. *Liao et al.* [1999] report on the effects of various types of aerosols on 14 tropospheric photolysis reactions, indicating that nonabsorbing aerosol generally enhances photolysis rates above and in the upper part of the aerosol layer, while soot and mineral aerosol reduce photolysis rates. *He and Carmichael* [1999] provide a sensitivity of photolysis rates and ozone production in the troposphere to aerosol properties using a coupled transport-chemistry-radiative transfer model, reporting reductions up to 70% to ground level ozone in the presence of absorbing aerosols in the boundary layer.

[6] Recently, results from the International Photolysis Frequency Measurement and Model Intercomparison (IPMMI) that was held in Boulder, Colorado, in June 1998 were presented [*Bais et al.*, 2000]. Seventeen radiative transfer models took part in the modeling exercise, while the photolysis frequencies were recorded at the surface by spectroradiometers, chemical actinometers, and broadband radiometers from eight groups. The comparison among measured photolysis rates showed that the majority of the instruments are in good agreement. For clear skies the comparability among different models depends strongly on wavelength and solar zenith angle, and these differences

are also reflected in the modeled J. The model calculations from the majority of the models were in good agreement for solar zenith angles <60°.

[7] Much limited knowledge exists on the photolysis rates over the photochemically active area of Eastern Mediterranean. As part of the Photochemical Activity and Solar Ultraviolet Radiation (PAUR) and PAUR II projects, two measuring campaigns took place in Greece. The first one took place in June 1996 on the small island of Agios Efstratios (39.57°N, 24.97°E) in the northern Aegean Sea and in Tatoi-Athens (38.11°N, 23.78°E). During that campaign key chemical compounds were measured [*Zerefos et al.*, 1998b; *Hofzumahaus and Hancock*, 1997], spectral measurements of UV irradiance were performed [*Kylling et al.*, 1998], in addition to measurements of the aerosol optical depth and the ozone profile [*Marenco et al.*, 1997]. Also airborne measurements of the actinic flux in the UV spectral region were performed over the Aegean Sea [*Hofzumahaus et al.*, 2002], as part of a joint PAUR-Altitude Dependence of the Tropospheric Ozone Photolysis (ATOP) experiment [*Zerefos et al.*, 1998b]. The second campaign (PAUR II) took place in Crete, Greece, during May 1999 [*Zerefos et al.*, 2002]. During this campaign, chemical compounds and the aerosol composition were measured at two different altitudes. In addition, at both sites, spectral measurements of the UV irradiance were performed, as well as measurements of the photolysis rates of $J(O^1D)$ and $J(NO_2)$.

[8] In this paper we compare radiative transfer model calculations of the actinic flux in the UV spectral region with airborne measurements of the actinic flux, obtained during the PAUR-ATOP campaign, in order to assess the accuracy of the model in calculating photolysis rates, when the model input parameters are well defined from the measurements. Next, the photolysis rates of $J(O^1D)$ and $J(NO_2)$ which were measured during PAUR II at two altitudes Gerani (35.53°N, 23.78°E, 30 m above sea level (asl)), and Prases (35.36°N, 23.85°E, 1000 m asl) are compared with the respective model calculations in order to examine the effect of the alternating aerosol composition (Sahara dust to maritime or urban aerosol) and of local environmental factors.

[9] The paper is organized in the following way: First, we give a brief description of the radiative transfer model used in this paper together with the model input parameters. Then we describe the source of the measured input parameters used for the calculations, as well the instrumentation used for the airborne measurements of the actinic flux and for the measurements of the photolysis rates. A brief description of the aerosol optical depth measurements used in this study follows. After that, for various altitudes in the troposphere the model calculations of the actinic flux are compared with the airborne measurements in order to justify its use for photolysis rates calculations. Finally, the model calculations of the photolysis rates are compared with the measurements obtained during PAUR II in order to investigate the effect of different aerosol environments on these measurements.

2. Data and Modeling

2.1. Radiative Transfer Model

[10] For the model calculations presented in this study the Tropospheric Ultraviolet and Visible (TUV) model was used [*Madronich*, 1993] (TUV version 4), which was available by anonymous ftp from S. Madronich, National Center for Atmospheric Research (NCAR). TUV includes different options for solving the radiative transfer equation, including various well-documented two-stream approximations as well as the discrete ordinate solver (DISORT) [*Stamnes et al.*, 1988]. In the version used, the pseudo-spherical approximation has also been incorporated [*Dahlback and Stamnes*, 1991]. In our calculations we used the DISORT with the pseudo-spherical approximation. Model and measured profiles for the atmospheric composition are used, which are scaled according to the observed O_3 and aerosol amounts. Rayleigh scattering by air molecules is calculated using the cross sections given by *Nicolet* [1984] and the air number density, as determined by the U.S. Standard Atmosphere (1976). Scattering by aerosols is calculated assuming a *Henyey and Greenstein* [1941] phase function, while the aerosol single scattering albedo and the asymmetry parameter are chosen from precalculated values by *Shettle and Fenn* [1979]. The spectral resolution used for the calculation was 0.05 nm and the ATLAS 3 Solar Ultraviolet Spectral Irradiance Monitor (SUSIM) extraterrestrial spectrum (M. E. Van Hoosier, personal communication, 1996) was adopted. The ozone cross sections were taken from *Bass and Paur* [1985]. The specific input parameters are discussed separately for each case the model has been applied in this study.

2.2. Spectral Actinic Flux Measurements

[11] For the validation of the TUV model, which was used in this study for the calculation of photolysis rates, we used spectral measurements of the downwelling and upwelling actinic flux, performed with a Bentham DTM 300 spectroradiometer [*Hofzumahaus et al.*, 1999] on board the DLR/Falcon aircraft on 10 June 1996 [*Hofzumahaus et al.*, 2002]. The measurements were performed in the frame of the joint PAUR-ATOP experiment, which took place in the north Aegean Sea during June 1996 [*Zerefos et al.*, 1998b]. The airborne measurements were performed on 10 June 1996 over the Aegean Sea across the track 40°N, 24°E to 30°N, 25°E, around solar noon. The measurements were performed at six cruising levels, in the altitude range between 100 and 12,000 m, which were held constant for 15 min. During this time, several UV spectra were recorded. The actinic flux spectra were measured with a resolution of 1 nm across the range 280–420 nm. The measurements were absolutely calibrated [*Hofzumahaus et al.*, 1999], and the wavelength calibration has been made using the Fraunhofer structure of the solar spectrum [*Huber et al.*, 1995; *Slaper et al.*, 1995] with an accuracy of 0.05 nm. The wavelength independent calibration error of the actinic flux is about ±6% [*Hofzumahaus et al.*, 1999]. The angular dependence of the detection sensitivity of the combined 4π sr system (one sensor looking downward and one sensor looking upward) is not perfectly isotropic and introduces an additional systematic error of <4%.

2.3. Measurements of $J(O^1D)$ and $J(NO_2)$ in Crete

[12] During the PAUR II campaign, two identical sets of instruments were operating continuously from 6 through 27 May 1999, at two sites, a high-altitude station (Prases, 1000 m) and a station at sea level (Gerani, 30 m). To measure

$J(NO_2)$, two-filter radiometers with isotropic input optics were used to determine the integrated photolysis rates providing 1-min analog signals including standard deviation. The spectral characteristics of these radiometers match the photolysis spectrum of the NO_2 molecule. The overall accuracy of the measurements is ~10%. To measure the photolysis rates of ozone, two single monochromators using a 512-pixel diode array detector were used, enabling synchronous sampling of all wavelengths in the spectrum. The spectrometers are constructed using monolithic ceramic blocks (focal length 110 mm) and are equipped with the same isotropic input optics. The characteristics of the spectrometers are full width half maximum (FWHM) 2.2 nm and pixel distance 0.83 nm. To account for the different light levels in the UVB, the UVA and the visible adapted integration times are used in these spectral ranges. The spectrum up to 325 nm is measured using an integration time of 5 s. The single spectral measurements are averaged to 1-min mean spectra. The error in the actinic flux determination due to photon flux calibration errors is 2.8%, and when propagated through to the determination of photolysis frequencies, an error in $J(O^1D)$ of 4% is obtained. The spectra are corrected for stray light (SL) and dark current (DC) by subtracting averages of the signals below 290 nm from the spectra recorded in the 290–450 nm region. This correction reduces the SL and DC error, which, for small zenith angles, is negligible for $\lambda > 325$ nm and between 2 and 5% for $\lambda < 325$ nm.

[13] At the beginning of the PAUR II experiment an intercomparison at the sea level site (6 and 7 May) of all radiometric instruments was arranged. The two spectroradiometers were independently calibrated. As an additional check the National Oceanic and Atmospheric Administration (NOAA) portable calibration was used on the Brewer and the Bentham. The filter radiometers used in PAUR II were calibrated using the long-term standard radiometers 505 and 720, which are compared to the chemical actinometer at the Forschungzentrum-Jülich, Germany, since 1992. For the calculation of the photolysis rates from the radiometric observations the following laboratory data sets were used. The quantum yield used for the determination of $J(O^1D)$ was taken from *Talukdar et al.* [1998]. The ozone absorption cross sections used were adopted from *Molina and Molina* [1986]. The quantum yield used for the determination of the $J(NO_2)$ were taken from *DeMore et al.* [1997], while the absorption cross sections were those determined by *Harder et al.* [1997].

2.4. Total Ozone and Aerosol Optical Depth Measurements

[14] Two double monochromator spectroradiometers were used for the determination of the total ozone amount and the aerosol optical depth during the campaign, one Bentham DTM 300, operated by the University of Innsbruck, and one Brewer MK III [*Bais et al.*, 1996], operated by the University of Thessaloniki. Both groups have participated in most of the recent spectroradiometer intercomparisons, and detailed descriptions of the characteristics of the instruments and on their accuracy can be found in the literature [e.g., *Gardiner and Kirsch*, 1995; *Bais et al.*, 2001]. The double Brewer spectroradiometer operated at the island of Agios Efstratios during PAUR and at the high-altitude site of Prases, Crete, during PAUR II. The total ozone measurements were performed according the standard Brewer routines [e.g., *Brewer*, 1973]. The aerosol optical depth τ in the UV region (290–366 nm) and the Ångstrom exponent α were determined by the methodology described by *Marenco et al.* [1997] on the basis of absolutely calibrated direct irradiance spectra [*Bais*, 1997]. The Bentham spectroradiometer operated during PAUR II at the low-altitude site of Gerani (30 m) and provided continuous total ozone and aerosol optical depth measurements based on direct Sun irradiance measurements in the wavelength range 290–420 nm [*Huber et al.*, 1995].

2.5. Lidar Measurements of Aerosol Backscattering Coefficient

[15] Measurements of the vertical distribution of the aerosol backscatter coefficient at 532 nm were performed during PAUR II at the sea level, near Gerani, by the Instituto di Fisica dell' Atmosfera, Consiglio Nazionale delle Ricerche (CNR), Italy, using a mobile, polarization lidar system based on a Nd-Yag pulsed laser source [*Gobbi et al.*, 2000]. Extinction coefficients were estimated by means of a statistical model describing the relationship between extinction and backscatter of both maritime and dust aerosols [*Barnaba and Gobbi*, 2001]. The integrated aerosol extinction (i.e., optical depths) in the layers 150 m to 1 km and 1–12 km have been used in this study to investigate the differences between the photolysis rates at the two sites, which can be attributed to the aerosols present within this layer.

3. Results and Discussion

3.1. Validation of the Radiative Transfer Model for Actinic Flux Calculations

[16] Simulated spectra of the total (4π sr) actinic flux were calculated with the TUV model, for all the measured spectra recorded on board the DLR Falcon on 10 June 1996. During that day, clear skies and low aerosol conditions prevailed over the Aegean Sea, providing a unique opportunity to describe the radiation field in the UV spectral region under well-defined clear-sky conditions. The model calculations were made using the DISORT solver of *Stamnes et al.* [1988], with the pseudo-spherical approximation [*Dahlback and Stamnes*, 1991], using 32 streams. The simulated spectra were calculated with 0.05-nm resolution, and then they were convolved with the slit function of the double monochromator, in the 290–405 nm spectral range. The solar zenith angle of each measured scan was taken into account in the calculations. The total ozone, used as input, was determined from the Brewer measurements at Agios Efstratios and was 344 Dobson units (1 DU = 2.69×10^{16} molecules cm^{-2}). The ozone profile was taken from the measurement performed at the airport of Thessaloniki, ~100 km northwest of the site [*Kylling et al.*, 1998] and scaled to the total ozone amount. The aerosol optical depth at 340 nm was set to 0.2, as determined by the Brewer [*Marenco et al.*, 1997], using *Elterman*'s [1968] profile for the vertical distribution of the aerosol extinction coefficient, scaled to the measured total aerosol optical depth. The single scattering albedo ω and the asymmetry parameter g were assumed to be 0.96 and 0.67, respectively, correspond-

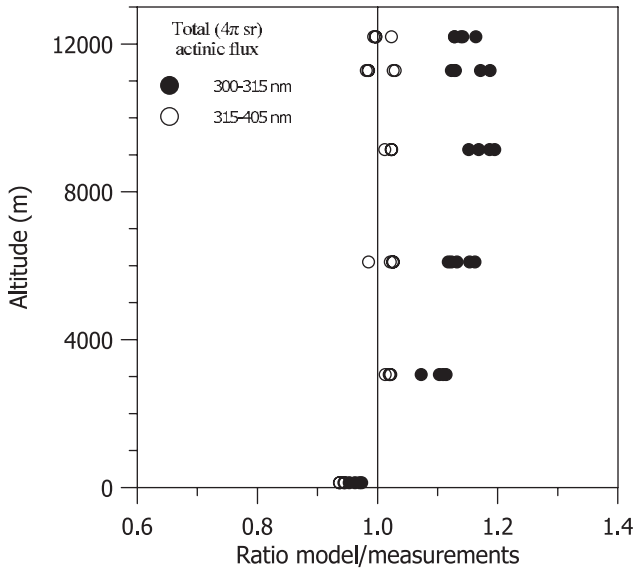

Figure 1. Mean ratio of calculated over 4π actinic fluxes, as a function of altitude for two spectral regions, 300–315 nm (solid circles) and 315–405 nm (open circles).

ing to theoretical calculations for a maritime aerosol model with 70% relative humidity [*Shettle and Fenn*, 1979]. The surface albedo was set to 5% in the whole 290–405 nm range. The range of the solar zenith angle for which the calculations were made ranged from 16° to 23°.

[17] In Figure 1 we present ratios of the modeled to the measured total actinic fluxes for the different altitudes at which measurements were taken. The ratios were calculated for the radiation integrated over the spectral intervals of 300–315 nm and 315–405 nm. The first interval corresponds to the UVB region that is strongly affected by the atmospheric ozone. The second interval corresponds to the UVA region and is less influenced by the ozone. In case of the UVA radiation the modeled and measured data agree well within ±3% at all altitudes (3–12 km), except for the lowest flight level (0.1 km) where the model is 6% lower than the measurements. The picture is different for the UVB radiation. In this case the ratio of 0.97 indicates good agreement at the lowest altitude but increases with altitude and reaches a maximum value of 1.17 at 9 km. The latter deviation is larger than the systematic errors in the measurements of the actinic flux. One explanation is the vertical ozone profile used as input in the model, but its measurement uncertainty cannot fully account for the observed differences. In addition, the assumed aerosol properties may cause errors in the model calculations. In another study, *Hofzumahaus et al.* [2002] compare the same experimental radiation data with the results from the UVSPEC model [*Kylling et al.*, 1998; *Mayer et al.*, 1997]. Different input parameters were used for the ground albedo (0.03) and the aerosol (vertical profile, single scattering albedo, and phase function), which were additionally constrained by ground-based lidar and irradiance measurements. As a result, the ratios of the modeled to measured spectral actinic fluxes are slightly smaller than the values in Figure 1 but show a similar trend versus altitude. The spectral UVSPEC data show agreement within ±5% in the UVA and ±10% in the UVB at high altitudes but underestimate the measured radiation by about 12% at the lowest flight level (0.1 km). Thus the agreement between modeled and experimental data is improved at higher altitudes, but the clear distinction in the magnitude of differences for the lowest and the higher altitudes is still present.

[18] The dependence of the UVB irradiance and/or actinic flux not only on the total ozone amount but also on its vertical distribution has been investigated by *Forster* [1995], where, for a fixed amount of total ozone, changes of as much as 17% in the irradiance at 305 nm have been reported. This magnitude of uncertainty allows the use of the model for the calculation of the photolysis rates of ozone and nitrogen dioxide, and their comparison with radiometrically determined measured rates, which as mentioned before, can be determined in the best case with an accuracy of 10%.

3.2. Variability of the Photolysis Rates of O_3 and NO_2 During PAUR II

[19] Figure 2 shows the daily and the day-to-day variability of the measured $J(O^1D)$ values at the two measuring sites, Prases (1000 m asl) and Gerani (30 m asl). There is a large day-to-day variability in the measurements, which is mostly determined by the large day-to-day variability in the total ozone measured during PAUR II [*Zerefos et al.*, 2002]. The local noon values ranged from 2.4×10^{-5} s^{-1} to 3×10^{-5} s^{-1} at Gerani and are larger at Prases, where the range is from 2.4×10^{-5} s^{-1} to 3.4×10^{-5} s^{-1}. There were no measurements available at Gerani on 15 May, and no long-term measurements are available in the area to compare with the measured values. The daily variability is strongly influenced by cloudiness, and this is also demonstrated in Figure 2. It should be noted here that the anticyclonic weather predominated in Crete throughout the campaign, with few interruptions [*Zerefos et al.*, 2002], which resulted to dry weather, mostly sunny at both places.

[20] Figure 3 shows the daily and the day-to-day variability of the measured $J(NO_2)$. The observed day-to-day variability is not so large during the days examined, and the main parameter that affects it is the aerosol loading, which was highly variable during that period [e.g., *Zerefos et al.*, 2002; *Gobbi et al.*, 2000; *Kouvarakis et al.*, 2002]. The local noon values ranged from 8×10^{-3} s^{-1} to 9.6×10^{-3} s^{-1} at Gerani and are larger at Prases, where the range is from 8.4×10^{-3} s^{-1} to 9.9×10^{-3} s^{-1}. These values are higher than the ones measured in Greece in June 1996 on the island of Agios Efstratios and in Athens [*Zerefos et al.*,

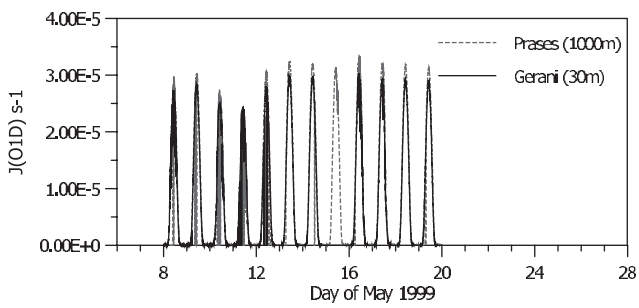

Figure 2. The variability of $J(O^1D)$ during the period 8–20 May 2000 at Prases (dashed line) and Gerani (solid line).

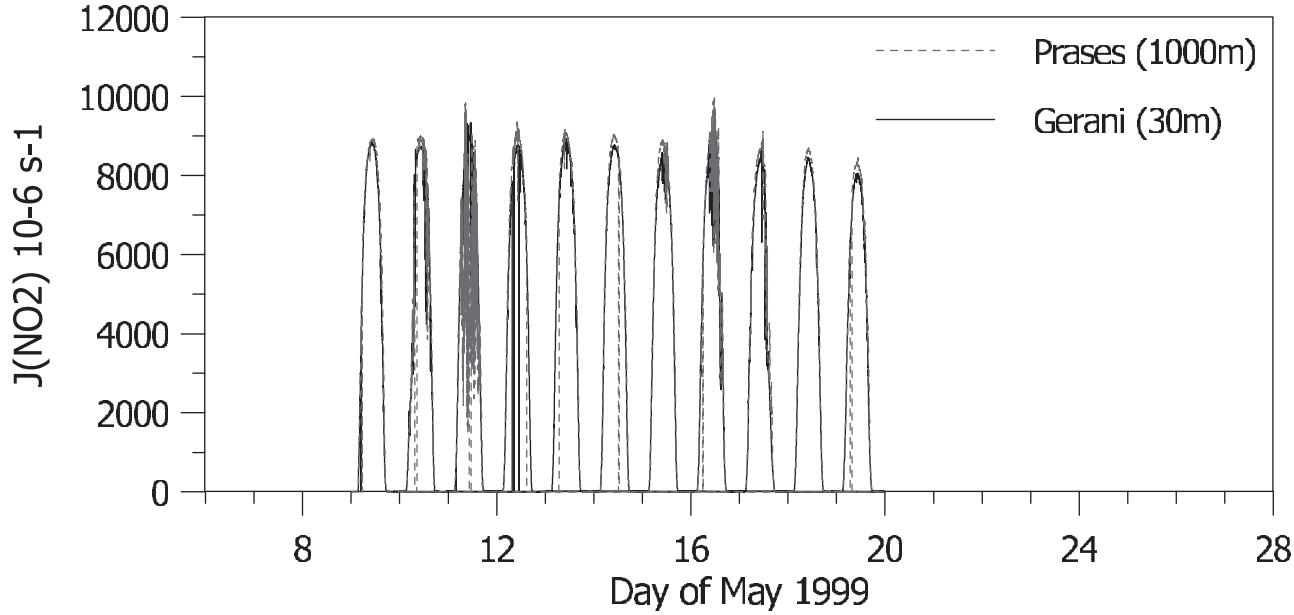

Figure 3. The variability of $J(NO_2)$ during the period 8–20 May 1999 at Prases (dashed line) and Gerani (solid line).

1998c]. The differential cloud cover between the two sites is also demonstrated in Figure 3.

[21] The observed variability of the local noon values will be discussed in detail in the sections 3.2.1 and 3.2.2.

3.2.1. Dependence of $J(O^1D)$ on Total Ozone and Aerosol Characteristics

[22] During the PAUR II experiment, large variability of the total ozone amount was detected at both sites [*Zerefos et al.*, 2002]. As it is demonstrated in Figure 4a, the total ozone at Gerani, as measured by the Bentham spectroradiometer, ranged from 306 to 414 DU and at Prases, as measured by the Brewer spectroradiometer, ranged from 295 to 390 DU. Similar variability was also measured by Earth Probe (EP) Total Ozone Mapping Spectrometer (TOMS). The aerosol loading as determined by the aerosol optical depth at 340 nm was also very variable during this period. As it is shown in Figure 4b, it ranged from 0.27 to 0.63 at Gerani and from 0.15 to 0.48 at Prases. The higher values of the aerosol optical depth measured during the period 17–20 May 1999 is the result of Sahara dust that was present above both measuring sites [*Gobbi et al.*, 2000]. The values shown in Figures 4a and 4b were used to calculate with the TUV model the corresponding to the measurements local noon values of $J(O^1D)$. The model setup was similar to the one used for validation in the previous paragraph, except that the vertical distribution of ozone and aerosol model profiles have been used [U.S. Standard Atmosphere, 1976; *Elterman*, 1968]. For the period 8–16 May for the single scattering albedo and asymmetry parameter we assumed a maritime aerosol model, where $\omega = 0.98$ and $g = 0.72$ [*Shettle and Fenn*, 1979], while for the Sahara dust event (17–20 May) according to *He and Carmichael* [1999], the corresponding values were set to $\omega = 0.77$ and $g = 0.77$. The Ångstrom exponent for the two periods was set to 1.5 and 0.5, respectively, as it was determined from the analysis of the direct Sun spectral measurements. For the calculation of $J(O^1D)$ from the actinic flux, TUV uses for the quantum yield the recommendation from *DeMore et al.* [1997] and the ozone absorption cross section from *Molina and Molina* [1986]. According to *Talukdar et al.* [1998] the J values calculated with the quantum yields recommended by *DeMore et al.* [1997] agree with those calcu-

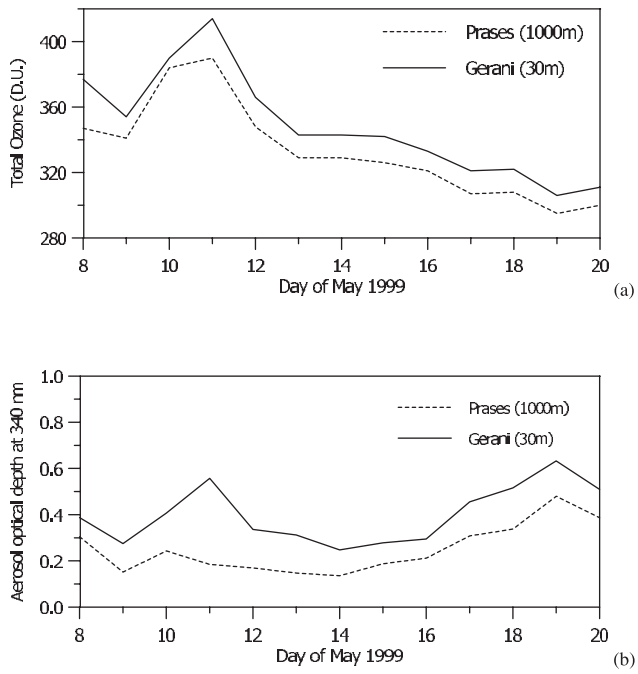

Figure 4. (a) Total ozone measurements at Prases (dashed line) and Gerani (solid line) used as input to the model calculations, for the period 8–20 May 1999. (b) Aerosol optical depth measurements at 340 nm at Prases (dashed line) and Gerani (solid line) used as input to the model calculations for the same period.

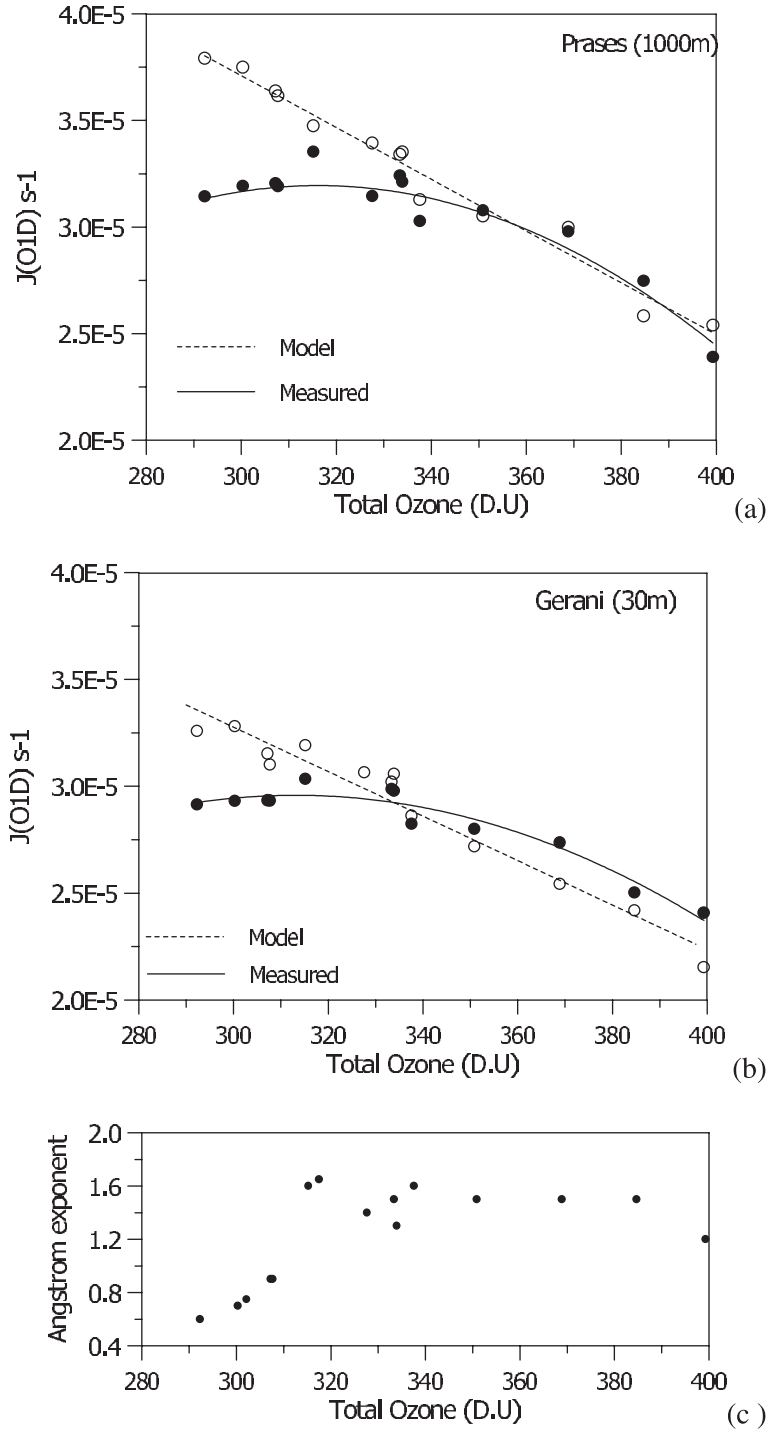

Figure 5. (a) The dependence of $J(O^1D)$ on total ozone as demonstrated by the model calculations (open circles) and the measurements (solid circles) for the Prases site. The dashed line is a linear fit and continuous line is second-degree polynomial fit. (b) Same as Figure 5a but for the Gerani site. (c) Corresponding Ångstrom exponent of the aerosol over the area.

lated with their quantum yields for zenith angles smaller than 40°, which is always the case in our calculation in this study. For all calculations, clear-sky conditions were considered.

[23] Figure 5a plots the local noon values of $J(O^1D)$ both measured and calculated versus the total ozone determined from EP TOMS for the high-altitude site. The model indicates that the J values increase almost linearly with decreasing total ozone. It has to be noted here that the solar zenith angle at local noon for the studied period did not vary significantly ranging between 18.5° and 15.6°. A similar pattern is demonstrated also from the measurements, but for

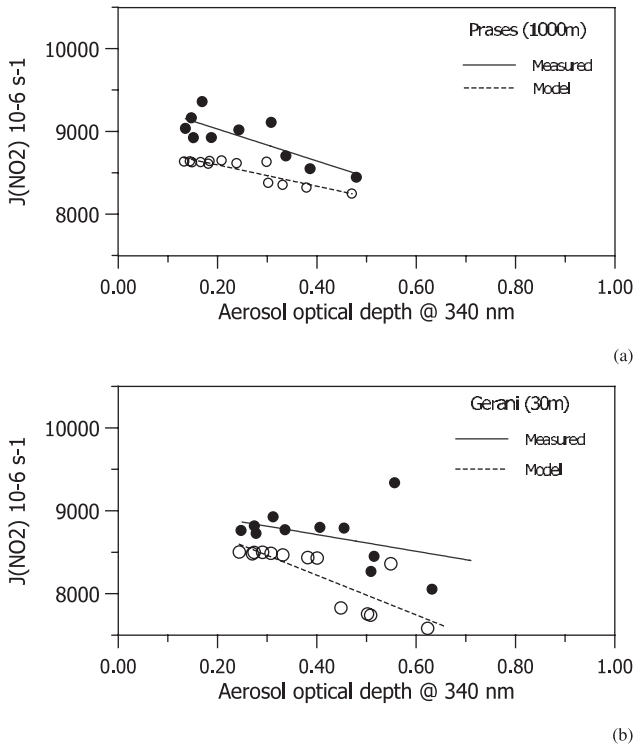

Figure 6. (a) The dependence of $J(NO_2)$ on aerosol optical depth as demonstrated by the model calculations (open circles) and the measurements (solid circles) for the Prases site. The dashed line and the continuous lines are linear fits. (b) Same as Figure 5a but for the Gerani site.

total ozone of <310 DU there is a plateau, or even a decrease of the $J(O^1D)$. For the specific zenith angle range this linear relationship leads to a radiation amplification factor (RAF), $(\Delta J/J)/(\Delta\Omega/\Omega)$, of ~1.5, which is larger than 1.1, the one calculated from long-term measurements of UV erythemal irradiance at Thessaloniki by *Zerefos et al.* [1998a]. The average ratio of the model values over the measurements is 1.06. If we consider only the values for total ozone >310 DU, then the ratio becomes 1.02, but for ozone values <310 DU it becomes 1.16. The same picture is demonstrated in Figure 5b but for the low-altitude site. For this case the ratio model-to-measurements is 1.01 for all cases, 0.98 for total ozone >310 DU, and 1.09 for the total ozone values <310. The differences between model and measurements that correspond to these ratios (0.98–1.09 and 1.02–1.16) are larger than the systematic errors involved in the experimental determination of the $J(O^1D)$. It should be stressed here that by chance the low total ozone values coincide with the high-aerosol (Sahara dust) event. This confirmed in Figure 5c, which shows the corresponding Ångstrom exponent for the local noon measurements of total ozone. Evidently, for total ozone >310 DU the average exponent is 1.5, which is representative for small particles (e.g., maritime or rural aerosols), while for the low ozone values the average exponent is ~0.7, which is representative for mineral dust [e.g., *Moulin et al.*, 1997]. These values correspond to the days, when Sahara dust was detected by the CNR lidar [*Gobbi et al.*, 2000], up to 10 km, and thus the days with low ozone values coincide with Sahara dust episodes. The measurements demonstrate that during intense dust episodes and high tropospheric ozone values, $J(O^1D)$ is lower even in comparison to days with higher total ozone. Based on the analysis of ozone profiles at Hohenpeissenberg, *Brühl and Crutzen* [1989] showed that decrease of UVB radiation at the Earth's surface is possible even when total ozone declines. They mention that especially for small zenith angles the tropospheric ozone absorbs UVB radiation more efficiently than stratospheric ozone because of an enhanced pathway through the atmosphere caused by Rayleigh and particle scattering. This hypothesis was tested here because these conditions (i.e., high tropospheric ozone of ~50 ppb [*Kourtidis et al.*, 2002] and intense Sahara dust episodes) were met during the PAUR II campaign and thus the observed decrease in the $J(O^1D)$ with decreasing total ozone can be explained by that mechanism. *He and Carmichael* [1999] point out that desert aerosols cause the largest decrease in photolysis rates, which is attributed to their backscattering and strongly absorbing properties, while *Liao et al.* [1999] note that desert dust reduces photolysis rates at all altitudes below the dust layer, with the largest reduction occurring in the dust layer itself. Although it takes into account multiple scattering, the radiative transfer model used could not simulate accurately this behavior.

3.2.2. Dependence of $J(NO_2)$ on Aerosol Characteristics

[24] Figure 6a plots the local noon values of $J(NO_2)$ both measured and calculated versus the aerosol optical depth at 340 nm for the Prases site. For the model calculation of the actinic flux we used the same setup as described previously. For the determination of the model-derived $J(NO_2)$, we used the quantum yield recommended by *Gardner et al.* [1987] and the used absorption cross section is from *DeMore et al.* [1997]. The ratio of the model-to-measurements is 0.94, which is within the uncertainty of both the measurements and the calculations. Both the measurements and the model show that for the small range of solar zenith angles considered here (18.5° to 15.6°), the increase in the aerosol optical depth causes a small decrease in $J(NO_2)$. The decrease is larger when Sahara dust particles are present, and this is consistent both in the calculations and in the measurements. The effect of the Sahara dust is enhanced in the low-altitude site of Gerani, as seen in Figure 6b, where the aerosol optical depth is systematically larger than in Prases. For this case the model-to-measurements ratio is also 0.94.

3.3. Altitude Effect on the Photolysis Rates

[25] Figure 7a shows the difference in $J(O^1D)$ between Prases and Gerani as calculated both from the measurements and the model. The measurements indicate that the difference between the two sites, which differ in altitude ~1 km, is rather constant of the order of 2.5×10^{-6} s^{-1}, which is ~10% of the values measured at Prases. The model-calculated difference is in agreement with the measurements for the period 9–16 May 1999, but the model overestimates this difference by 5% when the Sahara dust event is progressing. The overestimation by the model could be an indication that the aerosols within the first kilometer are not as absorbing as assumed in the model calculations and they consist of a mixture of nonabsorbing aerosol and dust [*Kouvarakis et al.*, 2002]. This assumption is verified by the model calculations (Figure 7a, solid line), since if we

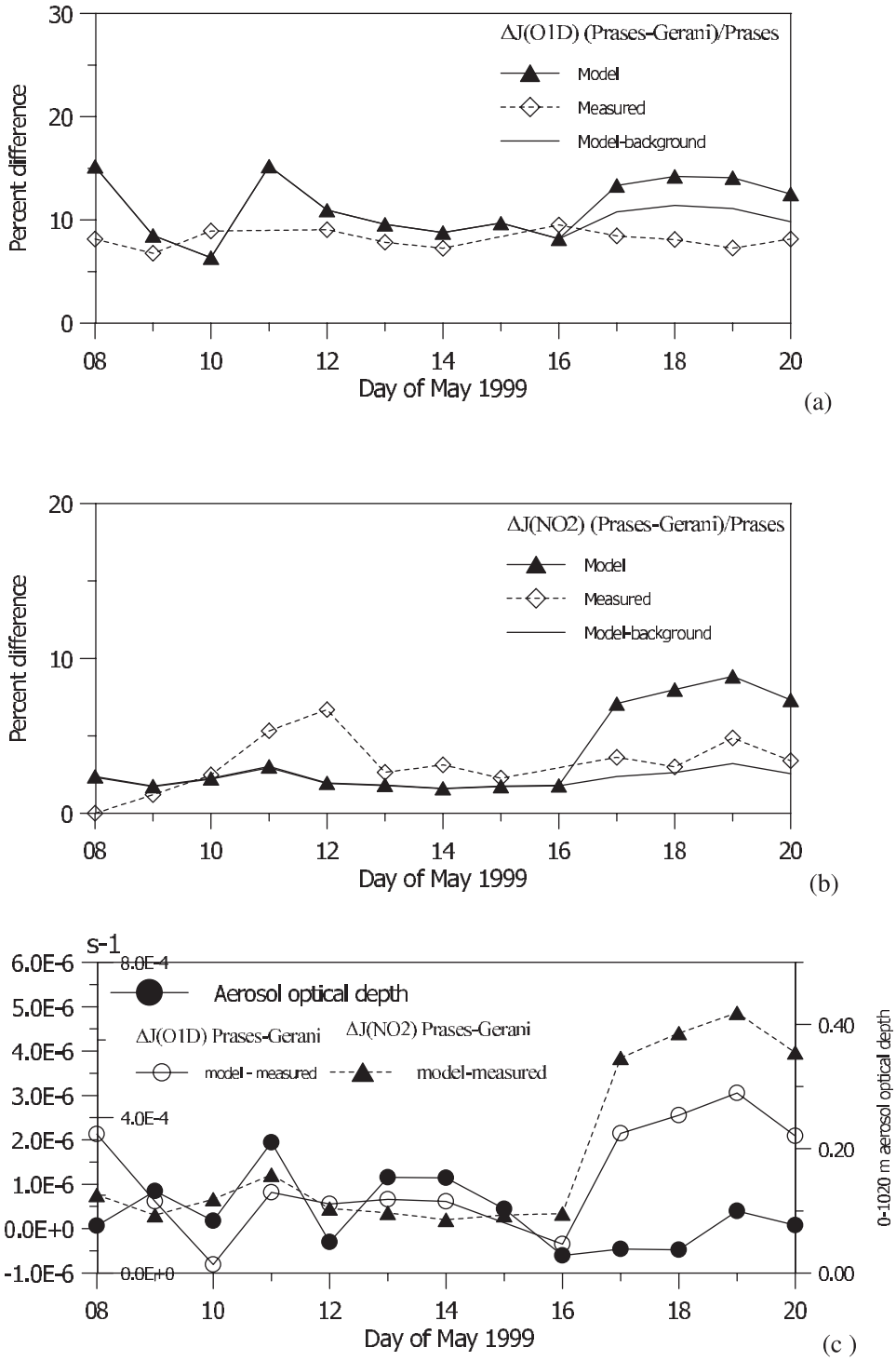

Figure 7. (a) Percent difference in the $J(O^1D)$ between Prases and Gerani, as calculated by the model (solid triangles) and by the measurements (open diamonds). (b) Percent difference in the $J(NO_2)$ between Prases and Gerani, as calculated by the model (solid triangles) and by the measurements (open diamonds). The solid lines indicate model calculations with background aerosol conditions. (c) Integrated aerosol optical depth determined by the lidar at 532 nm in the 0–1020 m layer (solid circles), the differences between model and measurements for the determination of $\Delta J(O^1D)$ (open circles) and $\Delta J(NO_2)$ (solid triangles) between Prases and Gerani.

assume background conditions (same as in the previous days) for the ω and g for these days, then the model estimates are much closer to the measured difference between the two sites. Three days backward trajectories presented by *Zerefos et al.* [2002] show that during the Sahara dust event the air masses arriving at 900 hPa over Crete originate from south Spain and central Italy, and thus the existence of nonabsorbing aerosol in this layer can be expected. The disagreement for 8 May is due to the large total ozone difference used as input for that day (see Figure 4a).

[26] Figure 7b shows the difference in $J(NO_2)$ between Prases and Gerani as calculated both from the measurements and the modeled values. There is a good agreement between the model- and measurement-calculated differences for the days with rather low aerosol optical over both sites (see Figure 4b) and the average difference due to altitude difference, is 0.3×10^{-3} s^{-1}, which is $\sim$3% of the values in Prases. During the Sahara dust event the model overestimates again the attenuation of solar UV radiation if we consider only absorbing aerosols within the first kilometer. Model estimates with background conditions for ω and g show better agreement, consistent with the discussion of Figure 7a.

[27] Apart from the absorbing properties of the aerosol in the first kilometer, another factor that may affect the difference of the J values between the two sites is the optical depth of the aerosols within this layer, assuming that above this layer the aerosol distribution is similar. In the model calculations we assumed that the aerosol optical depth in this layer follows the variability of the total aerosol optical depth, which is not always the case. Therefore part of the disagreement between the model and measurements in determining the altitude effect can be attributed to this assumption. The aerosol optical depth at 532 nm measured by the CNR lidar, integrated over the first kilometer, is shown in Figure 7c. This optical depth correlates well, for the non-Sahara aerosol days, with the photolysis rate difference between the high- and the low-altitude sites as determined by the model and the measurements shown in Figure 7c. For the Sahara dust event the lidar observations show that the lowermost aerosol layer (below 1 km), usually detected as liquid haze by the polarization channel, was observed to decrease [*Gobbi et al.*, 2000]. This situation resulted in the aerosol optical depth (AOD) residing mainly above 1 km during this period as opposed to the conditions recorded before, when the AOD over the first kilometer was of the same order of the AOD above 1 km altitude. Furthermore, during the dust event the lidar depolarization channel always observed a dominance of liquid particles below 1000 m altitude, while the depolarizing (nonspherical) dust particles dominated the backscatter above that altitude. Also, for these days the calculated differences follow the variation of the optical depth in this layer, but there is an overestimation from the model, when we assume only absorbing aerosols.

4. Conclusions

[28] The main results of the present work can be summarized as follows:

[29] Comparison of radiative transfer model calculations of actinic flux with airborne spectral actinic flux measurements indicates that the model can simulate the total actinic flux in the UVA region with an accuracy of 5% for the whole troposphere, when the modeling case is well defined. In the UVB region the uncertainty in the vertical distribution of ozone and aerosol can lead to differences, from 5–10% at low altitudes (<3 km) up to 20% at higher altitudes (>9 km).

[30] The agreement between modeled and measured photolysis rates of ozone and nitrogen dioxide at both sites examined is within 10%, when the uncertainty concerning the aerosol optical properties is small.

[31] For the small solar zenith angles examined, the predominant parameter that controls the variability of the photolysis rate of ozone is the total ozone content. However, high levels of tropospheric ozone and absorbing desert aerosols can cause a decrease in the photolysis rates of ozone, even under conditions of reduced total ozone content. This fact indicates that tropospheric ozone can be disproportionately important as a filter against UVB radiation when most scattering of the radiation by air molecules and dust occurs in the troposphere. Characteristically, the RAF for the $J(O^1D)$ is $\sim$1.5 and decreases in the presence of Sahara dust.

[32] The variability of the aerosol optical depth controls the variability of the $J(NO_2)$. The $J(NO_2)$ decreases in the presence of Sahara dust. This decrease is evident both in the measurements and in the model calculations. In contrast to the model/measurement differences seen in $J(O^1D)$, the comparison between modeled and measured $J(NO_2)$ is very good within the uncertainties involved. This strengthens the hypothesis of the role played by tropospheric ozone in the presence of absorbing aerosols.

[33] The overestimation by the model of the effect of the first kilometer layer relative to the measured difference between the two sites during the Sahara dust event indicates that there is a mixture of absorbing and nonabsorbing aerosols in this layer. The difference (ΔJ) between the photolysis rates at the high-altitude site and the low-altitude as determined by the model and the measurements correlates well with the integrated over the first kilometer aerosol optical depth at 532 nm measured by the lidar.

[34] **Acknowledgments.** The greater part of this work has been funded by the European Commission, Environment and Climate Programme, under contracts ENV4-CT95-0048, ENV4-CT95-158, and ENV4-CT97-0623.

References

Atkinson, R., et al., Evaluated kinetics and photochemical data for atmospheric chemistry: Supplement IV, *J. Phys. Chem. Ref. Data*, *21*, 1125–1568, 1992.

Bais, A. F., Absolute spectral measurements of direct solar ultraviolet irradiance with a Brewer spectrophotometer, *Appl. Opt.*, *36*, 5199–5204, 1997.

Bais, A. F., C. S. Zerefos, and C. T. McElroy, Solar UVB measurements with the double- and single-monochromator Brewer ozone spectrophotometers, *Geophys. Res. Lett.*, *23*, 833–836, 1996.

Bais, A. F., et al., An overview of the results from the International Photolysis Frequency Measurement and Model Intercomparison (IPMMI), paper presented at the International Radiation Symposium, Int. Radiat. Comm., St. Petersburg, Russia, 2000.

Bais, A. F., et al., SUSPEN intercomparison of ultraviolet spectroradiometers, *J. Geophys. Res.*, *106*, 12,509–12,526, 2001.

Ball, S. M., G. Hancock, S. E. Martin, and J. C. Pinot de Moira, A direct measurement of the $O(^1D)$ quantum yields from the photodissociation of ozone between 300 and 328 nm, *Chem. Phys. Lett.*, *264*, 531–538, 1997.

Barnaba, F., and G. P. Gobbi, Lidar estimation of tropospheric aerosol extinction, surface area and volume: Maritime and desert dust cases, *J. Geophys. Res.*, *106*, 3005–3018, 2001.

Bass, A. M., and R. J. Paur, The ultraviolet cross-section of ozone, I the measurements, in *Atmospheric Ozone: Proceedings of the Quadrennial Ozone Symposium*, edited by C. S. Zerefos and A. Ghazi, pp. 606–610, D. Reidel, Norwell, Mass., 1985.

Brewer, A. W., A replacement for the Dobson spectrophotometer, *Pure Appl. Geophys.*, *106–108*, 919–927, 1973.

Brühl, C., and P. Crutzen, On the disproportionate role of tropospheric ozone as a filter against solar UV-B radiation, *Geophys. Res. Lett.*, *16*, 703–706, 1989.

Castro, T., L. G. Ruiz-Suarez, J. C. Ruiz-Suarez, M. J. Molina, and M. Montero, Sensitivity analysis of UV radiation transfer model and experimental photolysis rates of NO_2, in the atmosphere of Mexico City, *Atmos. Environ.*, *31*, 609–620, 1997.

Dahlback, A., and K. Stamnes, A new spherical model for computing the radiation field available for photolysis and heating at twilight, *Planet. Space Sci.*, *39*, 671–683, 1991.

DeMore, W. B., et al., Chemical kinetics and photochemical data for use in stratospheric modeling, *Evaluation 11*, Jet Propul. Lab., Pasadena, Calif., 1994.

DeMore, W. B., et al., Chemical kinetics and photochemical data for use in stratospheric modeling, *Evaluation Number 12, JPL Publ., 97-4*, 1997.

Elterman, L., UV, visible and IR for altitudes to 50 km, *Rep. AFCR-68-0153*, Air Force Cambridge Res. Lab., Bedford, Mass., 1968.

Forster, P. M. D. F., Modeling ultraviolet radiation at the Earth's surface, part 1, The sensitivity of ultraviolet irradiances to atmospheric changes, *J. Appl. Meteorol.*, *34*, 2412–2425, 1995.

Gardiner, B. G., and P. J. Kirsch, Setting standards for European ultraviolet spectroradiometers, *Air Pollut. Res. Rep. 53*, 138 pp., Comm. of the Eur. Communities, Luxembourg, 1995.

Gardner, E. P., P. D. Sperry, and J. G. Calvert, Primary quantum yields of NO_2 photodissociation, *J. Geophys. Res.*, *92*, 6642–6652, 1987.

Gobbi, G. P., F. Barnaba, R. Giorgi, and A. Santacasa, Altitude-resolved properties of a Sharan dust event over the Mediterranean, *Atmos. Environ.*, *34*, 5119–5127, 2000.

Harder, J. W., J. W. Brault, P. V. Johnston, and G. H. Mount, Temperature-dependent NO_2 cross sections at high spectral resolution, *J. Geophys. Res.*, *102*, 3861–3879, 1997.

He, S., and G. R. Carmichael, Sensitivity of photolysis rates and ozone production in the troposphere to aerosol properties, *J. Geophys. Res.*, *104*, 26,307–26,324, 1999.

Henyey, L. G., and J. L. Greenstein, Diffuse radiation in the galaxy, *Astrophys, J.*, *93*, 70–83, 1941.

Hofzumahaus, A., and G. Hancock, Experimental study of the altitude dependence of the tropospheric ozone photolysis frequency between 0 and 12 km height (ATOP), *Final Rep. ENV4-CT95-0158 to European Commission*, Dir. Gen. XII, Programme Environ. and Clim., Brussels, Belgium, 1997.

Hofzumahaus, A., A. Kraus, and M. Müller, Solar actinic spectroradiometry: A technique for measuring photolysis frequencies in the atmosphere, *Appl. Opt.*, *38*, 4443–4460, 1999.

Hofzumahaus, A., A. Kraus, A. Kylling, and C. S. Zerefos, Solar actinic radiation (280–420 nm) in the cloud-free troposphere between ground and 12 km altitude: Measurements and model results, *J. Geophys. Res.*, *107*(DX), 10.1029/2001JD900142, 2002.

Huber, M., M. Blumthaler, W. Ambach, and J. Staehelin, Total atmospheric ozone determined from spectral measurements of direct solar UV irradiance, *Geophys. Res. Lett.*, *22*, 53–56, 1995.

Jacobson, M. Z., Studying the effects of aerosols on vertical photolysis rate coefficient and temperature profiles over an urban airshed, *J. Geophys. Res.*, *103*, 10,593–10,604, 1998.

Kerr, J. B., and C. T. McElroy, Evidence for large upward trends of ultraviolet-B radiation linked to ozone depletion, *Science*, *262*, 1032–1034, 1993.

Kourtidis, K. A., et al., Regional levels of ozone in the troposphere over eastern Mediterranean, *J. Geophys. Res.*, *107*(DX), 10.1029/2000JD000140, 2002.

Kouvarakis, G., Y. Doukelis, N. Mihalopoulos, S. Rapsomanikis, J. Sciare, and M. Blumthaler, Chemical, physical, and optical characterization of aerosols during PAUR II experiment, *J. Geophys. Res.*, *107*(DX), 10.1029/2000JD000291, 2002.

Kraus, A., and A. Hofzumahaus, Field measurements of atmospheric photolysis frequencies O_3, NO_2, HCHO, CH_3CHO, H_2O_2 and HONO by UV spectroradiometry, *J. Atmos. Chem.*, *31*, 161–180, 1998.

Kraus, A., F. Rohrer, and A. Hofzumahaus, Intercomparison of NO_2 photolysis frequency measurements by actinic flux spectroradiometry and chemical actinometry during JCOM97, *Geophys. Res. Lett.*, *27*, 1115–1118, 2000.

Krol, M. C., and M. van Weele, Implications of variations in photodissociation rates for global tropospheric chemistry, *Atmos. Environ.*, *31*, 1257–1273, 1997.

Kylling, A., A. F. Bais, M. Blumthaler, J. Schreder, C. S. Zerefos, and E. Kosmidis, Effect of aerosol on solar UV irradiances during the Photochemical Activity and Solar Ultraviolet Radiation campaign, *J. Geophys. Res*, *103*, 26,051–26,060, 1998.

Lantz, K. O., R. E. Shetter, C. A. Cantrell, S. J. Flocke, J. G. Calvert, and S. Madronich, Theoretical, actinometric, and radiometric determinations of the photolysis rate coefficient of NO_2 during the Mauna Loa Observatory Experiment 2, *J. Geophys. Res.*, *101*, 14,613–14,629, 1996.

Liao, H., Y. L. Yung, and J. H. Seinfeld, Effects of aerosols on tropospheric rates in clear and cloudy atmospheres, *J. Geophys. Res.*, *104*, 23,697–23,707, 1999.

Madronich, S., UV radiation in the natural and perturbed atmosphere, in *Environmental Effects of Ultraviolet Radiation*, edited by M. Tevini, pp. 17–69, Lewis, Boca Raton, Fla., 1993.

Madronich, S., and C. Granier, Tropospheric chemistry changes due to increased UV-B radiation, in *Stratospheric Ozone Depletion/UV-B Radiation in the Biosphere*, edited by R. H. Biggs and M. E. B. Joyner, pp. 1–10, Springer-Verlag, New York, 1994.

Marenco, F., V. Santacesaria, A. Bais, D. Balis, A. Di Sarra, A. Papayannis, and C. S. Zerefos, Optical properties of tropospheric aerosols determined by lidar and spectrophotometric measurements (PAUR campaign), *Appl. Opt.*, *36*, 6875–6886, 1997.

Mayer, B., G. Seckmeyer, and A. Kylling, Systematic long-term comparison of spectral UV measurements and UVSPEC modeling results, *J. Geophys. Res.*, *102*, 8755–8767, 1997.

McElroy, C. T., C. Midwinter, D. V. Barton, and R. B. Hall, A comparison of *J*-values from composition and photodissociative flux measurement with model calculation, *Geophys. Res. Lett.*, *22*, 1365–1368, 1995.

Michelsen, H. A., R. J. Salawitch, P. O. Wennberg, and J. G. Anderson, Production of $O(^1D)$ from photolysis of O_3, *Geophys. Res. Lett.*, *21*, 2227–2230, 1994.

Molina, L. T., and M. J. Molina, Absolute absorption cross section of ozone in the 185–350 nm wavelength range, *J. Geophys. Res.*, *91*, 14,501–14,508, 1986.

Moulin, C., F. Guillard, F. Dulac, and C. E. Lambert, Long-term daily monitoring of Saharan dust load over ocean using Meteosat ISCCP-B2 data, 1, Methodology and preliminary results for 1983–1994 in the Mediterranean, *J. Geophys. Res.*, *102*, 16,947–16,958, 1997.

Müller, M., A. Kraus, and A. Hofzumahaus, $O(^1D)$ photolysis frequencies determined from spectroradiometric measurements of solar actinic UV-radiation: Comparison with chemical actinometer measurements, *Geophys. Res. Lett.*, *22*, 679–682, 1995.

Nicolet, M., On the molecular scattering in the terrestrial atmosphere: An empirical formula for its calculation in the homosphere, *Planet. Space Sci.*, *32*, 1467–1468, 1984.

Ruggaber, A., R. Dlugi, A. Bott, R. Forkel, H. Herrmann, and H.-W. Jacobi, Modeling of radiation quantities and photolysis frequencies in the aqueous phase in the troposphere, *Atmos. Environ.*, *31*, 3137–3150, 1997.

Seckmeyer, G., B. Mayer, G. Bernhard, R. Erb, A. Aldbold, H. Jaeger, and W. R. Stockwell, New maximum UV irradiance levels observed in central Europe, *Atmos. Environ.*, *31*, 2971–2976, 1997.

Shetter, R. E., et al., Actinometric and radiometric measurement and modeling of the photolysis rate coefficient of ozone to $O(^1D)$ during the Mauna Loa Observatory Experiment 2, *J. Geophys. Res.*, *101*, 14,631–14,641, 1996.

Shettle, E. P., and R. W. Fenn, Models for the aerosols of the lower atmosphere and effects of humidity variations on their optical properties, *Environ. Pap. 676*, Air Force Geophys. Lab., Bedford, Mass., 1979.

Silvente, E., R. C. Richter, M. Zheng, E. S. Saltzman, and A. J. Hynes, Relative quantum yields of O^1D production in the photolysis of ozone between 301 and 336 nm: Evidence for the participation of a spin-forbidden channel, *Chem. Phys. Lett.*, *264*, 309–315, 1997.

Slaper, H., H. A. J. M. Reinen, M. Blumthaler, M. Huber, and F. Kuik, Comparing ground-level spectrally resolved solar UV measurements using various instruments: A technique resolving effects of wavelength shift and slit width, *Geophys. Res. Lett.*, *22*, 2721–2724, 1995.

Stamnes, K., S. C. Tsay, W. J. Wiscombe, and K. Jayaweera, Numerically stable algorithm for discrete-ordinate-method radiative transfer in multiple scattering and emitting layered media, *Appl. Opt.*, *27*, 2502–2509, 1988.

Takahashi, K., Y. Matsumi, and M. Kawasaki, Photodissociation processes of ozone in the Huggins Band at 308–326 nm: Direct observation of $O(^1D_2)$ and $O(^3P_j)$ products, *J. Phys. Chem.*, *100*, 4084–4089, 1996.

Talukdar, R. K., C. A. Longfellow, M. K. Giles, and A. R. Ravishankara,

Quantum yields of O(^1D) in the photolysis of ozone between 289 and 329 nm as a function of temperature, *Geophys. Res. Lett.*, *25*, 143–146, 1998.

World Meteorological Organization, Scientific Assessment of Ozone Depletion: 1998, in *Global Ozone Research and Monitoring Project Report, Rep. 44*, Geneva, 1999.

Zerefos, C. S., D. S. Balis, A. F. Bais, D. Gillotay, P. C. Simon, B. Mayer, and G. Seckmeyer, Variability of UV-B at four stations in Europe, *Geophys. Res. Lett.*, *24*, 1363–1366, 1997.

Zerefos, C. S., C. Meleti, D. Balis, K. Tourpali, and A. F. Bais, Quasi-biennial and longer-term changes in clear sky UV-B solar irradiance, *Geophys. Res. Lett.*, *25*, 4345–4348, 1998a.

Zerefos, C. S., et al., Overview of results from PAUR campaign, paper presented at the European Conference on Atmospheric UV Radiation, Eur. Comm. and Finn. Meteorol. Inst., Helsinki, Finland, 29 June to 2 July 1998b.

Zerefos, C. S., et al., Photochemical Activity and Solar Ultraviolet Radiation (PAUR), *Final Rep. ENV4-CT95-0048 to European Commission*, Dir. Gen. XII, Programme Environ. and Clim., Brussels, Belgium, 1998c.

Zerefos, C. S., et al., Photochemical Activity and Solar Ultraviolet Radiation Modulation Factors (PAUR): An overview of the project, *J. Geophys. Res.*, *107*(DX), 10.1029/2000JD000134, 2002.

A. F. Bais, D. S. Balis, K. Kourtidis, and C. S. Zerefos, Laboratory of Atmospheric Physics, Physics Department, Aristotle University of Thessaloniki, Campus Box 149, Thessaloniki 54006, Greece. (balis@auth.gr; kourtidi@auth.gr; zerefos@olymp.ccf.auth.gr)

M. Blumthaler, Institute of Medical Physics, University of Innsbruck, Muellerstrasse 44, A-6020 Innsbruck, Austria. (mario.blumthaler@uibk.ac.at)

G. P. Gobbi, Instituto di Fisica Dell' Atmosfera, CNR, Via Fosso del Cavaliere 100, Rome I-00133, Italy. (gobbi@sunifa1.ifsi.rm.cnr.it)

A. Hofzumahaus, Institute for Atmospheric Chemistry, Forschungzentrum Juelich, Postfach 1913, Julich D-52425, Germany. (a.hofzumahaus@kfa-juelich.de)

A. Kraus, Gruenenthal GmbH, P.O. Box 500444, D-52088 Aachen, Germany. (Al.Kraus@kfa-juelich.de)

R. Schmitt, Meteorologie Consult GmbH, Auf der Platt 47, D-61479 Glashuetten, Germany. (metcon@Compuserve.com)